Radiotherapy and Oncology xxx (2014) xxx–xxx

Contents lists available at ScienceDirect

Radiotherapy and Oncology

journal homepage: www.thegreenjournal.com

Original article

Validation of the mid-position strategy for lung tumors in helical TomoTherapy

Marie Wanet [a], Edmond Sterpin [a], Guillaume Janssens [a], Antoine Delor [b], John Aldo Lee [a], Xavier Geets [a,b,*]

[a] Center of Molecular Imaging, Radiotherapy and Oncology, Institut de recherche expérimentale et clinique, Université catholique de Louvain; and [b] Department of Radiation Oncology, Cliniques universitaires Saint-Luc, Brussels, Belgium

ARTICLE INFO

Article history:
Received 6 August 2013
Received in revised form 18 October 2013
Accepted 20 October 2013
Available online xxxx

Keywords:
Lung cancer
Tumor motion
TomoTherapy
Monte Carlo simulation
Geometric uncertainties

ABSTRACT

Purpose: To compare the mid-position (MidP) strategy to the conventional internal target volume (ITV) for lung tumor management in helical TomoTherapy, using 4D Monte Carlo (MC) plan simulations.

Materials and methods: For NSCLC patients treated by SBRT ($n = 8$) or SIB-IMRT ($n = 7$), target volumes and OARs were delineated on a contrast-enhanced CT, while 4D-CT was used to generate either ITV or MidP volumes with deformable registrations. PTV margins were added. Conformity indexes, volumetric and dosimetric parameters were compared for both strategies. Dose distributions were also computed using a 4D MC model (TomoPen) to assess how intra-fraction tumor motion affects tumor coverage, with and without interplay effect.

Results: PTVs derived from MidP were on average 1.2 times smaller than those from ITV, leading to lower doses to OARs. Planned dose conformity to TVs was similar for both strategies.

4D MC computation showed that ITV ensured adequate TV coverage (D_{95} within 1% of clinical requirements), while MidP failed in 3 patients of the SBRT group (D_{95} to the TV lowered by 4.35%, 2.16% and 2.61%) due to interplay effect in one case and to breathing motion alone in the others.

Conclusions: Compared to the ITV, the MidP significantly reduced PTV and doses to OARs. MidP is safe for helical delivery except for very small tumors (<5 cc) with large-amplitude motion (>10 mm) where the ITV might remain the most adequate approach.

Helical TomoTherapy is an appealing irradiation modality to treat unresectable locally advanced stage II–III as well as inoperable stage I non-small cell lung cancer (NSCLC) patients. Indeed, it combines an advanced technique of intensity-modulated radiation therapy (IMRT), leading to highly conformal dose distributions, with an accurate imaging device for patient positioning, based on megavoltage computed tomography (MVCT). These features allow target volumes to be irradiated with sharp dose gradient, and thus help deliver high dose while sparing healthy surrounding tissues.

However, tumor motion caused by breathing may jeopardize treatment quality. In that regard, on-line management of respiratory tumor motion requires dedicated methodologies and techniques, like breath hold, gating [1], or tracking [2], which are not yet available in TomoTherapy systems [3]. Thus, treatment plan robustness against breathing motion still relies on the definition of specific volumes, like an internal target volume (ITV) or the mid-position (MidP), which are expanded with safety margins.

The ITV approach is widely used in clinical practice [4–6]. The ITV encompasses all tumor positions during the breathing cycle and can be determined from a four-dimensional computed tomography (4D-CT). A planning study with four-dimensional (4D) Monte Carlo (MC) has demonstrated that an expanded ITV can be safely applied in TomoTherapy [3]. In particular, interplay effect between beam and tumor motions did not significantly affect the delivered dose distributions. However, the ITV approach is known to overestimate the safety margins, and thus may lead to unnecessary irradiation of healthy tissues [7,8].

The MidP, on the other hand, involves a volume that corresponds to the time-weighted mean position of target volumes during the breathing cycle [8]. This approach provides several theoretical advantages over the ITV and partly overcome the issues encountered with the ITV. First, by using a 4D-CT, it eliminates the systematic error that would otherwise occur with a fast 3D CT that is merely a snapshot at some point of the respiratory cycle, possibly polluted by artifacts. In contrast with the ITV approach, the random uncertainty about tumor motion is added in quadrature to the other random geometric uncertainties in the formula for the Planning Target Volume (PTV) margin calculation proposed by van Herk et al. [9]. As a result, this approach allows the margins to be significantly smaller and therefore comparable to those obtained with gated radiotherapy [8]. Furthermore, the MidP approach allows the treatment planning and delivery workflow to remain the same as in other approaches based on margins.

* Corresponding author. Address: Department of Radiation Oncology, Cliniques Universitaires Saint-Luc, Avenue Hippocrate, 10, B-1200 Brussels, Belgium.
E-mail address: xavier.geets@uclouvain.be (X. Geets).

0167-8140/$ - see front matter © 2013 Elsevier Ireland Ltd. All rights reserved.
http://dx.doi.org/10.1016/j.radonc.2013.10.025

To our best knowledge, MidP has never been implemented for helical TomoTherapy of moving lung tumors, nor compared to ITV for this treatment modality. In this context, we designed the present study to assess the potential gain of MidP over ITV in terms of margin and PTV reduction. As a second objective, we investigated whether these volumetric changes in the PTV actually lowered the irradiation of the organs at risk using clinically relevant dosimetric parameters. Finally, we also computed motion-corrected dose distributions for both scenarios using a previously validated 4D Monte Carlo (MC) model based on TomoPen [3]. The latter was used to assess the plan quality, especially the potential impact of intra-fraction motion and treatment delivery mechanics on tumor coverage when margins were reduced.

Materials and methods

Fig. 1 illustrates the complete workflow from image acquisitions to treatment planning.

Patient selection

Fifteen NSCLC patients were retrospectively included in the present study. Among these, 8 patients had stage I NSCLC treated with stereotactic body radiation therapy (SBRT), while the remaining 7 patients had locally-advanced stage II–III NSCLC treated with simultaneous integrated boost (SIB) IMRT in the framework of a dose escalation protocol. The internal review board approved this study and all patients gave their informed consent.

Image acquisition

Prior to treatment, all patients underwent a planning imaging session either on a big bore CT scanner (Aquilion LB, Toshiba medical system corporation, Japan) or a combined PET-CT scanner (Gemini TF, Philips Medical system, Cleveland, OH, USA). For all acquisitions, patients were immobilized in a thermoformed plastic mask (CIVCO Medical Solutions, Iowa, USA).

A contrast-enhanced CT (CE-CT) from the entire thoracic region was acquired in free breathing mode for the purpose of delineation, and reconstructed in 2 mm-thick slices. Next, a 4D-CT was acquired and patients were audio-coached to regularize their breathing and thus reduce 4D-CT image artefacts [10,11]. In this acquisition mode, the CT scanner automatically set the optimal helical pitch according to the patient's breathing period measured from either a pressure belt (Medspira/Mayo Clinic Breath Hold™, Mayo Clinic Medical Devices, USA) or magnetic sensors (Nomics©, Liège, Belgium). The 4D-CT datasets were retrospectively binned into 10 equally distributed temporal phases, for motion management purposes. Finally, an average CT was computed by averaging all 10 phases.

For the SIB group, 4D-FDG-PET images were also acquired 60–120 min after injection of an average activity of 8.04 mCi of FDG in patients fasting at least for 6 h before examination. The breathing signal was recorded with the same devices as the 4D-CT. After correction for decay, random, scatter, and attenuation, images were reconstructed with the iterative algorithm 3D LOR-OSEM. The images had a transverse FOV of 180 mm (one bed position centered on the region of interest). The attenuation correction was performed using the averaged 4D-CT.

Motion estimation

Internal motion due to breathing was estimated with the 4D-CT images. First, the CE-CT and the end-exhale phase of the 4D-CT were non-rigidly registered using a log-domain diffeomorphic Morphon algorithm (see Appendix for more details). This method is based on the matching of the local phase (i.e., lines and edges) at different scales and is therefore insensitive to contrast differences between the CE-CT and the 4D-CT. Next, this registration algorithm was run to map the end-exhale phase of the 4D-CT with the other phases, yielding 9 non-rigid transformations [12]. The latter were used in two different ways: first, to compute the deformation between the reference phase and the mean position of the anatomy along the respiratory cycle, which will further be applied to the CE-CT-based target volumes (TVs) to generate their corresponding MidP volumes and, second, to propagate these contours on all other phases of the respiratory cycle, the union of all deformed TVs forming an individual ITV. The deformed contours were visually checked on all phases, to assess registration accuracy. For the SIB group, the combined PET/CT acquisitions allowed MidP PET images to be computed in a straightforward way, just by applying the non-rigid deformations to the PET component.

Definition of target volumes and organs at risk

For both the ITV and MidP, Fig. 1 illustrates the workflow for the definition of the target volumes (TVs) and organs at risk (OARs). It comprises the following steps:

(1) OARs, gross tumor volume (GTV_{CT}) and clinical target volume (CTV_{CT}) of primary tumors and lymph nodes were manually delineated on the CE-CT. As there is no CTV extension for the SBRT group (i.e., $CTV_{CT} = GTV_{CT}$), the GTV will be noted CTV in the rest of the text, for the sake of clarity [13,14]. Additionally, for the SIB group, a GTV_{PET}, corresponding to the boost region, was automatically segmented on PET images using a previously validated gradient-based method [15,16].
(2) The corresponding ITV_{CT} and ITV_{PET} were generated using non-rigid registration, like previously described.
(3) Then, the internal structures were computed in their mid-position, using the transformation vectors from deformable registrations as described earlier. The resulting TVs were noted $GTV_{CT\text{-}MidP}$, $CTV_{CT\text{-}MidP}$ and $GTV_{PET\text{-}MidP}$.
(4) The PTV margins were drawn using the formalism proposed by van Herk et al.

In the last step, the margin thickness formula combines different types of geometric uncertainties and can be written as

$$M_{PTV} = 2.5\sqrt{\left(\Sigma_{TM}^2 + \Sigma_{BL}^2 + \Sigma_{SETUP}^2 + \Sigma_D^2\right)} + 1.64 \times \sqrt{\left(\sigma_{TM}^2 + \sigma_{BL}^2 + \sigma_{SETUP}^2 + \sigma_p^2\right)} - 1.64\sigma_p,$$

where Σ and σ denote the standard deviations of the systematic and random errors, respectively. Subscripts TM, BL, SETUP, D and p refer to tumor motion, baseline shift, patient setup variability, delineation uncertainty, and penumbra, respectively. The coefficients in the formula ensure that the CTV receives at least 95% of the prescribed dose for 90% of patients. All standard deviations, except Σ_{TM} and σ_{TM}, were set in agreement with the literature, while also taking into account the specificities of TomoTherapy and the handling of operators in our treatment unit [17–19]. These values were similar for ITV and MidP. In the particular case of penumbra, its width σ_p for helical TomoTherapy was computed as follows. Dose profiles in transverse and longitudinal directions at 5 cm depth for a 5×5 cm^2 field were obtained with TomoPen MC simulations in a 0.33 g/cm^3 density phantom. The computed profile was fitted with the sum of two Gaussians according to Witte et al. [20]. The effect of couch motion on dose distributions can be approximated as a convolution of the beam with a square response with

Please cite this article in press as: Wanet M et al. Validation of the mid-position strategy for lung tumors in helical TomoTherapy. Radiother Oncol (2014), http://dx.doi.org/10.1016/j.radonc.2013.10.025

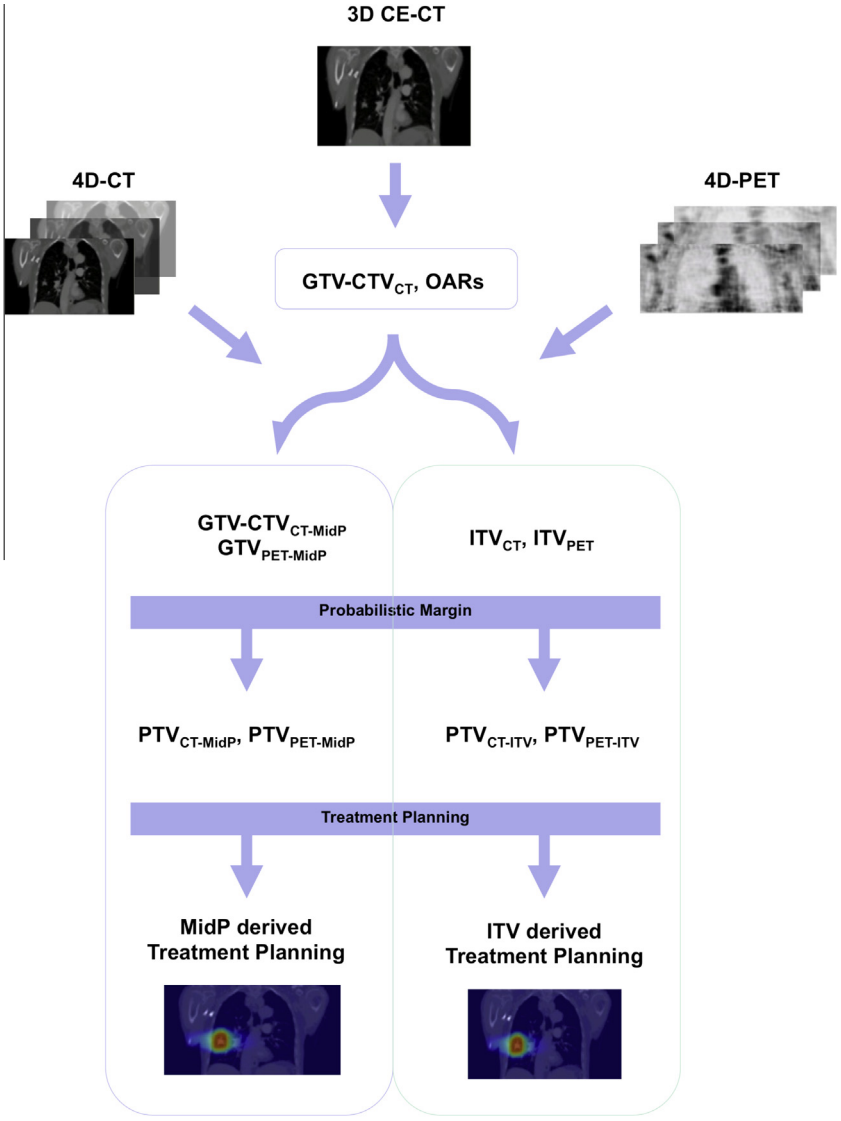

Fig. 1. Workflow depicting the definition of target volumes and organs at risk for ITV and mid-position strategies from the image acquisition to the treatment planning.

SW width, SW being the slice width. The standard deviation related to the couch motion equals $\frac{SW}{\sqrt{12}}$. The total standard deviation was computed, leading to σ_p adapted for lung density and TomoTherapy delivery. In the end, σ_p equaled 4.6 and 4.3 mm in LR and AP directions. For the SI direction, it corresponded to 4.3 and 9 mm for the 1 or 2.5 cm slice widths, respectively.

Last but not least, standard deviations related to tumor motion were individually estimated, depending on the considered margin strategy:

- For the ITV, the tumor motion uncertainties are implicitly included in the ITV margin, which encompasses the CTV deformed onto the different respiratory phases of the 4D-CT [21]. Both Σ_{TM} and σ_{TM} were therefore set to 0 [8].
- For the MidP, Σ_{TM} was fixed to 0.5 mm, which corresponds to the residual error of deformable registration [8], whereas σ_{TM} was particularized according to the amplitudes of tumor motion measured in the 4D-CT along each axis [8,19].

Table 1 provides volumetric information for the GTVs and CTVs, their motion along each axis, as well as the PTV margins for both ITV and MidP approaches. It is noteworthy that primary tumor and lymph nodes move differently but, for the sake of clarity, Table 1 does not report this information.

Treatment planning

For each patient, two treatments were planned, either with an ITV or a MidP.

For the SBRT group, a dose of 54 Gy in 3 fractions to the PTV was prescribed, except for two patients who received 60 and 48 Gy in 4 fractions due to the proximity between their tumor and critical mediastinal structures. For the SIB group, a dose of 62.5 Gy was prescribed to the PTV of the primary tumor defined on CT images (PTV_{T-CT}) and the PTV of the lymph nodes defined on CT images (PTV_{N-CT}), and delivered in 25 fractions of 2.5 Gy. Simultaneously, a higher dose was individually prescribed to the PTV_{PET} based on the maximal tolerance of each organ at risk [22]. These doses were prescribed to 95% and 50% of the PTV for SBRT and SIB treatment groups respectively, according to RTOG 0236 and 0618 trials and ICRU83 recommendations [13,23–25].

Treatment plans were performed on a research version of the TomoTherapy Treatment Planning System (TPS). Its new dose engine, performing computations on a general-purpose graphical

Please cite this article in press as: Wanet M et al. Validation of the mid-position strategy for lung tumors in helical TomoTherapy. Radiother Oncol (2014), http://dx.doi.org/10.1016/j.radonc.2013.10.025

Table 1
GTV and CTV with their corresponding motion amplitudes and PTV margins for both ITV and MidP approaches. Patients 1–8 correspond to the SBRT group (i.e., GTV = CTV) and patients 9–15 correspond to the SIB treatment group.

Pat. No.	$CTV_{T\text{-}CT}$ (cc)	$CTV_{N\text{-}CT}$ (cc)	GTV_{PET} (cc)	LR motion (mm)	AP motion (mm)	SI motion (mm)	PTV_{MidP} LR margins (mm)	PTV_{MidP} AP margins (mm)	PTV_{MidP} SI margins (mm)	PTV_{ITV} LR margins (mm)	PTV_{ITV} AP margins (mm)	PTV_{ITV} SI margins (mm)
1	2.8	–	–	1.7	7.5	8.0	5.7	10.2	10.0	5.5	8.7	8.5
2	4.8	–	–	5.3	8.1	8.5	6.3	10.0	9.9	5.5	8.7	8.5
3	12.2	–	–	0.8	0.6	2.0	5.7	8.8	8.7	5.5	8.7	8.5
4	2.5	–	–	3.2	3.3	10.8	6.2	9.5	9.6	5.5	8.7	8.5
5	10.5	–	–	5.2	11.8	30.0	6.3	11.0	20.9	5.5	8.7	8.5
6	5.2	–	–	2.1	7.5	10.3	5.8	9.8	10.9	5.5	8.7	8.5
7	10.9	–	–	1.4	2.4	7.5	5.7	8.9	9.1	5.5	8.7	8.5
8	3.5	–	–	2.2	3.8	24.6	5.8	9.1	18.3	5.5	8.7	8.5
9	183.8	–	88.7	1.3	1.5	2.1	5.7	8.8	8.4	5.5	8.7	8.2
10	122.1	66.8	61.0	0.4	2.3	2.0	5.7	8.9	8.4	5.5	8.7	8.2
11	29.3	34.1	8.9	1.0	3.7	4.2	5.7	9.1	8.6	5.5	8.7	8.2
12	212.0	38.4	57.3	0.3	1.7	0.7	5.7	8.8	8.3	5.5	8.7	8.2
13	319.9	24.5	187.5	0.4	1.3	5.9	5.5	8.7	8.7	5.5	8.7	8.2
14	99.0	29.5	39.6	1.2	2.4	5.4	5.7	8.9	8.7	5.5	8.7	8.2
15	137.6	–	63.6	1.0	4.3	12.0	5.7	9.2	10.1	5.5	8.7	8.2

Abbreviations: $CTV_{T\text{-}CT}$ and $CTV_{N\text{-}CT}$, clinical target volume of the primary tumor and the lymph nodes on CT images, respectively; GTV_{PET}, gross tumor volume of the primary tumor on PET images; LR, left–right; AP, anterior–posterior; SI, superior–inferior; PTV_{MidP} and PTV_{ITV} margin, planning target volume margins derived from the mid-position and the internal target volume approaches, respectively.

processing unit, showed excellent agreement with former versions running on conventional central processors, and was previously validated for heterogeneous media on phantoms and patient cases [26,27]. For SBRT patients, treatment plans were generated using a fine dose grid, a 1 cm field width, a pitch ranging from 0.172 to 0.215, and a planned modulation factor (ranging from 1.2 to 1.5) adapted in order to obtain a gantry period below 60 s (required by the TPS) and a treatment time short enough to keep the patient setup variability as low as possible. For SIB treatment patients, all plans were generated using a 2.5 cm field width, a pitch of 0.287 and a planned modulation factor of 2.0.

Treatment planning was performed on the average CT. Although the CE-CT acquired in free breathing offers the optimal contrast for delineation purpose, it only represents a snapshot of the patient's anatomy at a given time point, and may suffer from motion-related artefacts. On the contrary, the average CT represents a voxel-wise average of the ten 4D-CT phases and therefore adequately renders the mean geometry and density of the patient [28–30].

The evaluation of treatment plan quality relied on constraints to TVs and OARs. In the SBRT group, constraints on the PTV were set as follows in an overlapping mode: D_{95} equals the prescription dose; D_{99} above 90% of the prescribed dose; D_2 within a range of 110–140% of the prescribed dose according to RTOG recommendations [24,25]. Constraints to the OARs were also set according to these trials [24,25]. In the SIB group, the acceptability criteria for TVs, in an overlapping mode, were: D_{50} equals prescribed dose for both the PTV_{CT} and PTV_{PET}, a D_{95} above 95% of the prescribed dose, a D_{99} above 90% of the prescribed dose and a D_2 below 105% of the prescribed dose for the PTV_{PET}. The physical dose constraints for the OARs, taken from the literature [31–41], were normalized for the prescribed dose (i.e., 62.5 Gy given in 25 fractions) and equivalent doses in 2 Gy per fraction (EQD2) using the appropriate α/β values were calculated with the LQ-model for each parameter.

MC simulations with TomoPen

In the case of dynamic IMRT delivery, patient and beam motions may interfere, potentially resulting in a distortion of the dose distributions, i.e., the so-called interplay effect [42]. Dose distributions were computed using a previously validated 4D MC model based on TomoPen, in order to assess the impact of intra-fraction tumor motion on tumor coverage, with and without the interplay effect [43–46]. TomoPen was used to:

(1) Recompute the 3D dose distributions, comparable to the planned dose generated with TomoTherapy's TPS and denoted 3D MC planned doses hereafter.
(2) Compute 4D dose distributions for every 4D-CT data set, with or without beamlet-phase correlation, that is, with interplay simulation (4D MC IS) or no interplay (4D MC NI) [3,47].

The 4D MC model was previously described in [3]. The simulated dose maps with and without interplay were compared with MC dose distributions computed on the average CT used for planning.

It is noteworthy that the 4D MC doses include the effect of motion, in contrast to the 3D MC planned dose. As a consequence, 4D MC doses must be assessed with smaller volumes whose margins account for all uncertainties but tumor motion. In other words, GTVs and CTVs are expanded differently, isotropically and with $\Sigma_{TM} = 0$ and $\sigma_{TM} = 0$, into volumes called GTV_{PET}^{exp} and CTV_{CT}^{exp}, to be compared to the PTVs in the 3D MC doses.

Finally, the impact of tumor motion and interplay on tumor dose coverage was quantified by comparing the different dose–volume histogram (DVH) metrics obtained for the 3D MC planned dose and the 4D MC doses with and without interplay. Firstly, D_{mean}, D_{99}, D_{95}, and D_2 were computed for the 3D MC planned dose distribution in the PTVs. Secondly, these metrics were computed for 4D MC dose distributions with and without interplay on the modified GTV and CTV volumes (GTV_{PET}^{exp} and CTV_{CT}^{exp}). Basically, the various DVH metrics in the PTV for the 3D MC planned dose distributions were compared to the same metrics in the GTV_{PET}^{exp} and CTV_{CT}^{exp} drawn on the 4D MC dose distributions with and without interplay. Afterward, DVH metrics for 4D MC doses with or without interplay were compared to single out the potential interplay effect alone.

Statistical evaluation

PTVs expanded from the MidP and ITV were compared in terms of volumes. Dosimetric parameters (mean ± standard deviation) for TVs and OARs were computed and compared between the MidP and ITV treatment plans. Likewise, plan conformity indexes were calculated and compared between plans. The Paddick conformity index is defined as $CI_{Paddick} = \frac{TV_{PI}^2}{TV \times PI}$ where TV_{PI} is the target volume (TV) within the prescribed isodose volume (PI). Dice's similarity index is defined as $DSI = \frac{2 \times TV_{PI}}{TV+PI}$. A perfect plan would have TV_{PI} = PI = TV and therefore $CI_{Paddick} = 1$ and DSI = 1 [48–50].

Please cite this article in press as: Wanet M et al. Validation of the mid-position strategy for lung tumors in helical TomoTherapy. Radiother Oncol (2014), http://dx.doi.org/10.1016/j.radonc.2013.10.025

All the statistical calculations were performed with NCSS software 2004© (Number Cruncher Statistical System, Kaysville, UT, USA), p-values lower than 0.05 were considered statistically significant and all tests were two-sided. Doses and volumes were pairwise compared between ITV and MidP using either Student t-tests when data were normally distributed, or Wilcoxon signed rank tests for non-Gaussian distributions.

Results

Volumetric analysis

The PTVs expressed in cc are reported in Table 2. The PTVs expanded from the ITV were on average 1.2 times larger than those obtained with the MidP. This difference was statistically significant for both the SBRT and the SIB groups (t-test, $p < 0.001$ and $p = 0.027$, respectively).

Dosimetric analysis for OARs

Smaller PTVs allowed MidP to outperform the ITV by delivering less dose to each OAR (see Table 3). In the SBRT group, the differences were statistically significant for the mean lung dose (MLD) and $V_{20\ Gy}$, D_2 for the spinal cord, D_2 and $V_{30\ Gy}$ for the thoracic wall, and finally D_2 for the esophagus. In the SIB group, the differences were statistically significant for $V_{20\ Gy}$ for the lungs-GTV, $V_{25\ Gy}$ for the heart, D_{mean} for the esophagus, and D_2 for the main bronchi.

Dosimetric analysis for TVs

The MidP and ITV plans significantly differed for TVs parameters, with p-values ranging between 0.04 and 0.006 for D_{mean}, D_{99}, D_{95} and D_2 to the PTV. However, these differences were inferior to 1%, except for D_{95} in the SIB group, where it is inferior to 4% due to the higher dose in the boosted sub-volume of the

Table 2
PTV corresponding to the primary tumors, lymph nodes and PET-based boost expressed in cc for mid-position and ITV plans for all patients. The ratios between ITV and MidP derived PTV are also presented.

Patient No.		$PTV_{T\text{-}CT}$ (cc)			$PTV_{N\text{-}CT}$ (cc)			PTV_{PET} (cc)		
		MidP	ITV	Ratio	MidP	ITV	Ratio	MidP	ITV	Ratio
SBRT	1	24.6	33.3	1.36	–	–	–	–	–	–
	2	33.9	48.2	1.42	–	–	–	–	–	–
	3	52.8	57.9	1.10	–	–	–	–	–	–
	4	20.3	31.7	1.56	–	–	–	–	–	–
	5	84.5	95.1	1.13	–	–	–	–	–	–
	6	38.6	50.5	1.31	–	–	–	–	–	–
	7	48.2	63.2	1.31	–	–	–	–	–	–
	8	36.5	46.2	1.26	–	–	–	–	–	–
	Mean	42.4	53.3	1.31	–	–	–	–	–	–
	SD	20.2	20.1	0.15	–	–	–	–	–	–
SIB	9	396.6	443.7	1.12	–	–	–	212.7	214.5	1.01
	10	270.4	295.6	1.09	210.0	251.7	1.20	120.7	128.3	1.06
	11	90.6	109.1	1.20	140.6	184.3	1.31	29.0	37.8	1.30
	12	533.9	627.8	1.18	153.3	194.6	1.27	72.3	72.8	1.01
	13	591.0	668.5	1.13	97.7	122.2	1.25	312.2	337.3	1.08
	14	259.4	313.7	1.21	118.5	147.4	1.24	66.5	74.1	1.11
	15	358.9	459.4	1.28	-	-	-	105.0	126.9	1.21
	Mean	357.3	416.8	1.17	144.0	180.0	1.25	131.2	141.7	1.11
	SD	171.1	196.0	0.06	42.6	49.4	0.04	98.6	103.4	0.11

Abbreviations: MidP, mid-position; ITV, internal target volume; SD, standard deviation.

Table 3
Comparison of dosimetric metrics for the OARs (mean ± SD) between treatment plans with MidP and ITV.

OARs	Parameters		SIB			p-Value	SBRT			p-Value
			MidP (mean ± SD)	ITV (mean ± SD)	Δ (mean ± SD)		MidP (mean ± SD)	ITV (mean ± SD)	Δ (mean ± SD)	
Lungs-GTV	MLD	(Gy)	15.86 ± 1.48	16.57 ± 1.43	0.72 ± 0.87	0.072	3.70 ± 1.24	4.00 ± 1.24	0.30 ± 0.23	0.008
	Bio MLD	(Gy)	14.57 ± 1.74	15.33 ± 1.43	0.76 ± 0.74	0.035	–	–	–	–
	$V_{20\ Gy}$	(%)	25.29 ± 2.97	27.00 ± 3.47	1.71 ± 1.69	0.028	5.04 ± 2.33	5.55 ± 2.27	0.51 ± 0.22	<0.001
Spinal cord	D_2	(Gy)	28.77 ± 5.73	33.07 ± 7.41	4.30 ± 8.48	0.23	7.20 ± 3.33	7.89 ± 3.42	0.70 ± 0.70	0.025
Heart	D_2	(Gy)	–	–	–	–	7.02 ± 7.75	7.83 ± 8.48	0.80 ± 1.01	0.06
	$V_{25\ Gy}$	(%)	11.62 ± 8.36	14.92 ± 11.07	3.31 ± 2.87	0.023	–	–	–	–
Esophagus	D_2	(Gy)	–	–	–	–	40.70 ± 14.92	42.52 ± 15.15	1.82 ± 1.24	0.018
	D_{mean}	(Gy)	24.47 ± 9.32	26.33 ± 9.47	1.86 ± 0.63	<0.001	–	–	–	–
	D_{max}	(Gy)	68.26 ± 14.08	70.11 ± 10.98	1.85 ± 4.35	0.31	–	–	–	–
Rib cage	D_2	(Gy)	–	–	–	–	14.29 ± 10.41	17.14 ± 10.42	2.85 ± 2.42	0.004
	$V_{30\ Gy}$	(cc)	–	–	–	–	10.91 ± 5.58	12.14 ± 6.16	1.22 ± 1.12	0.013
Vessels	D_2	(Gy)	70.65 ± 9.25	71.59 ± 8.22	0.94 ± 1.42	0.12	–	–	–	–
Bronchus	D_2	(Gy)	75.51 ± 9.25	76.48 ± 9.35	0.75 ± 0.45	0.005	–	–	–	–

Abbreviations: OARs, organs at risk; SIB, simultaneous integrated boost; SBRT, stereotactic body radiation therapy; MidP, mid-position; ITV, internal target volume; Δ, difference between ITV and MidP values; MLD, mean lung dose; V_xGy, volume of the OAR receiving x Gy; D_x, dose received by x percent of the OAR volume.

Please cite this article in press as: Wanet M et al. Validation of the mid-position strategy for lung tumors in helical TomoTherapy. Radiother Oncol (2014), http://dx.doi.org/10.1016/j.radonc.2013.10.025

PTV; this higher difference was not clinically relevant. Notwithstanding, the mean conformity indexes computed for the MidP and ITV plans were similar in the SBRT group (Paddick of 0.84 ± 0.05 with $p = 0.92$, DSI of 0.92 ± 0.03 with $p = 0.91$), and did not significantly differ in the SIB group, with Paddick of 0.67 ± 0.23 and 0.62 ± 0.23 ($p = 0.20$), and DSI of 0.80 ± 0.18 and 0.76 ± 0.18 ($p = 0.24$), for MidP and ITV plans respectively. This showed that both the ITV and MidP plans were similar enough in terms of PTV coverage to be further compared.

MC simulations

Fig. 2 reports for each patient the relative difference (in percent) for D_{95} between the 3D MC planned dose distributions and the "interplay simulated" or "no interplay" dose distributions for the primary TVs (note that nodes and boost volumes are not illustrated) used to assess the plans quality. A table compiling all the different metrics, i.e., D_{mean}, D_{99}, D_{95} and D_2 for primary tumors, nodes and boost volumes, is included in the Appendix.

For all SBRT patients, D_{mean}, D_{99}, D_{95}, and D_2 of the 4D MC dose in CTV_{CT}^{exp} complied with the planning recommendations when using the ITV approach. In particular, tumor motion and interplay effect did not degrade the plan quality.

In contrast, MidP failed to adequately cover CTV_{CT}^{exp} in 3 patients. For patient 5, the simulated interplay effect decreased D_{99} and D_{95} in CTV_{CT}^{exp} by 7.20% and 4.35%, respectively, compared to the planned dose distributions (Fig. 3a). Although the interplay effect did not affect the two other patients, MC simulations demonstrated significant underdosages of CTV_{CT}^{exp}, compared to the planned doses, with D_{mean}, D_{99}, and D_{95} reduced by 1.90%, 2.16%,

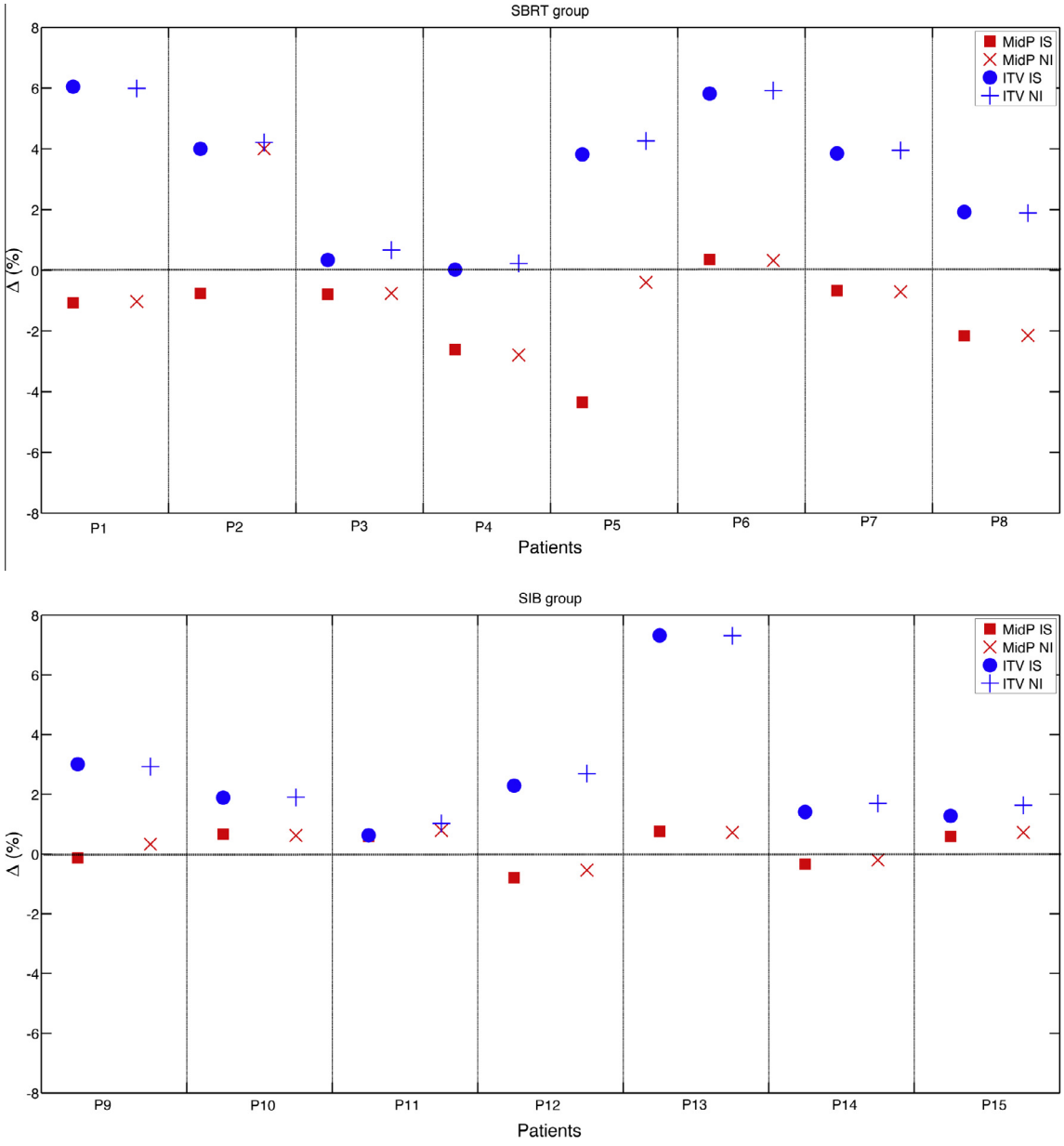

Fig. 2. Relative difference (Δ) for D_{95} to the CT based primary target volume (CTV_{CT}^{exp}) between the 3D Monte Carlo (MC) planned dose distributions and Interplay Simulated (IS) or No Interplay (NI) dose distributions calculated using a 4D MC model for mid-position and ITV strategies for SBRT (a) and SIB group (b). In the former case, it is important to note that ITV approach ensures adequate tumor coverage for all patients. In contrast, MidP strategy do not guarantee sufficient dose coverage to the CTV_{CT}^{exp} in 3 patients. For P5, the reduction of dose coverage to the CTV_{CT}^{exp} is due to the interplay effect. For P4 and P8, the significant underdosage to the CTV_{CT}^{exp} arises from the breathing motion alone. For the SIB group, both strategies ensure adequate tumor coverage for all patients. Neither tumor motion nor the interplay effect degrades the plan quality.

Please cite this article in press as: Wanet M et al. Validation of the mid-position strategy for lung tumors in helical TomoTherapy. Radiother Oncol (2014), http://dx.doi.org/10.1016/j.radonc.2013.10.025

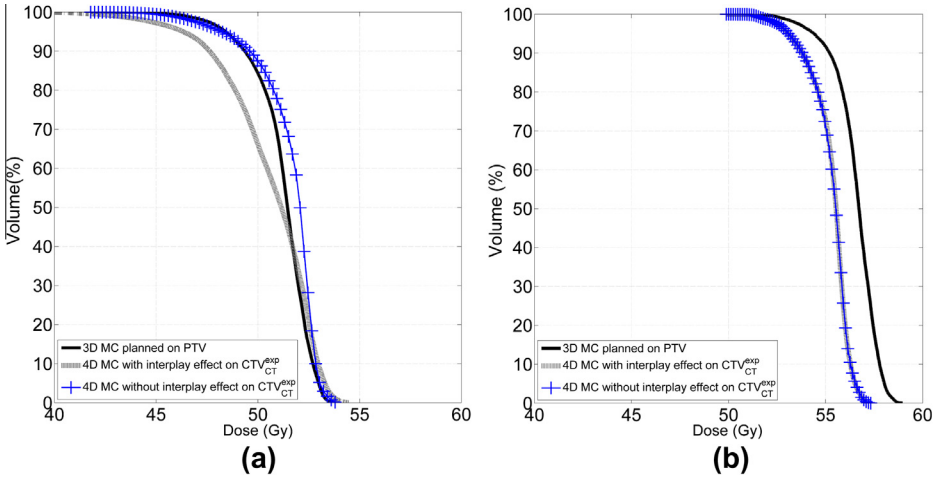

Fig. 3. Dose–volume histograms (DVHs) representing the planned dose on the planning target volume (PTV) and the actual delivered doses calculated with and without the interplay effect on the expanded gross tumor volume CTV^{exp}_{CT} for patient 5 (a) and patient 8 (b).

and 2.61% for patient 4 and by 2.52%, 1.36%, and 2.16% for patient 8, respectively (Fig. 3b).

For all SIB patients, D_{mean}, D_{99}, D_{95} and D_2 to the CTV^{exp}_{CT} and GTV^{exp}_{PET} computed from 4D MC dose distributions complied with the planning recommendations when using both approaches. In particular, it is important to note that neither the tumor motion nor the interplay effect affect the plan quality. On the other hand, a significant tumor coverage improvement to the CTV^{exp}_{CT} was observed in 4D MC computed plans compared to the 3D planned MC ones when ITV approach was used in both SIB and SBRT groups (see Fig. 2).

Discussion

Our study confirmed that the MidP leads to significantly smaller PTVs than the ITV, which also translated into lower doses delivered to the OARs. Although the dose reduction may seem modest at first sight, it matters in the context of hypofractionated RT schemes with high biologically equivalent doses. As all plans were made in a similar way by the same person and showed comparable dose conformities to the PTV, the differences in dose distributions to OARs are believed to faithfully reflect volumetric changes.

Based on these observations, the MidP appears as an appealing option for motion management in lung cancer treatment with TomoTherapy. A MidP volume can be derived for any moving structure, such as the primary tumor, lymph nodes, or even tumor sub-volumes. Moreover, MidP is easy to implement in clinical routine because it affects only the target volumes definition, and leaves all other aspects of planning unchanged; MidP does not require neither any additional equipment in the treatment room, nor complex 4D features in the TPS. It only entails the computation of the target volumes in their time-weighted average position, using a 4D-CT scan whose phases are non-rigidly registered. Unfortunately, no commercial implementation of MidP exists at the moment, which hinders adoption in clinical routine.

The most innovative aspect of our study was the MC verification of the dose distributions in the target volumes for both the ITV and MidP. In agreement with our previous study [3], the 4D MC simulations confirmed that the ITV ensured adequate dose coverage to CTV^{exp}_{CT} in all cases. Overdosage in CTV^{exp}_{CT} observed in 4D MC plans was mainly attributable to the intrinsic overestimation of motion in the calculation of the PTV margin with the ITV. This improved D_{95} compared to the PTV without motion. For the CTV^{exp}_{CT} in the SIB group, additional overdosage may also stem from the use of two prescription levels on a moving target, with a substantial portion of the CTV entering the high dose region defined by the PTV_{PET}, especially for P11, P13 and P15 with SI motion as large as 12 mm.

In contrast, 4D MC simulations indicated that the MidP strategy did not guarantee sufficient dose coverage to the CTV^{exp}_{CT} in 3 out of 15 cases, all in the SBRT group. In the first case (P5), underdosage resulted from the interplay effect, which is specific to TomoTherapy and manifests in the form of undesired hot and cold spots within the TVs, comparable to constructive and destructive interferences. It results from a delivering fluence different from the planned fluence when respiratory intra-fraction motion and couch progression take place in TomoTherapy delivery. Kissick et al. showed that these hot and cold spots are minimized when the jaw width is large and scanning velocity is small relatively to the breathing amplitude and frequency [51,52]. For this patient, we used the smallest jaw width (1.0 cm) and a couch pitch of 0.215. Moreover, the patient breathing period was 6 s, and tumor motion was particularly large, with displacements of 5.16, 11.81 and 29.97 mm in LR, AP and SI directions, respectively. Finally, our MC simulations calculated only one fraction of the treatment, which maximizes the interplay effect. Previous studies showed that interplay effect tends to average out after multiple fractions [51,53]. However, the small number of fractions, only 4 here, limits this advantageous effect.

In both other cases (P4 and P8), the significant agreement between 4D MC dose distributions with and without interplay suggested that breathing motion alone was responsible for the degradation of the DVHs. Possible reasons are simplifications introduced in the PTV margin formula:

(1) Spherical GTVs were assumed while most tumors deviate from this shape. Moreover, the formula ignores the GTV size and shape as long as it is large compared to random errors (σ) [9]. However, in these two cases, the tumor volumes were very small with GTV of about 3 cc and 1.5 cm diameter in both cases, thus questioning the applicability of the model.
(2) Rotations and shape variations of the tumor have been disregarded in the model. Nonetheless, in these cases, we could expect that rotational errors be most likely of minor clinical importance given the limited size and quite regular shape of the considered tumors [54–56].

Please cite this article in press as: Wanet M et al. Validation of the mid-position strategy for lung tumors in helical TomoTherapy. Radiother Oncol (2014), http://dx.doi.org/10.1016/j.radonc.2013.10.025

(3) The margin formula assumes Gaussian distributions for all geometric errors, on the basis of the central limit theorem [9]. If this theorem applies, convolving the dose with a Gaussian distribution can simulate the global effect of geometric uncertainties on dose distributions. However, breathing motion may easily depart from normality and hence invalidate the whole formula if the contribution of tumor motion is large compared to other source of uncertainties.

The first and third hypotheses are not met in P4 and P8. Indeed, P4 and P8 had very small tumors (2.48 and 3.49 cc) combined with large tumor motion (10.84 and 24.63 mm of displacement in the SI directions, see also Table 1). In comparison, the penumbras for SBRT patients were 4.6, 4.6, and 4.3 mm in the LR, AP, and SI directions, thus undermining the applicability of the central limit theorem for those patients. In this context, P4 and P8 deviate from the formalism of van Herk et al. and one might expect the MidP to underestimate the presence of the tumor at both ends of its trajectory, thereby jeopardizing coverage.

From a pragmatic point of view, simple rules based on tumor size and motion amplitude could be applied to choose between both margin strategies: the MidP should be privileged against the ITV since it allows for significant TV and dose reduction, except in tumors showing simultaneously small size (i.e., below 1.5 cm) and large motion amplitude (i.e., above 1 cm). In this scenario, the benefit of margin reduction should be weighed against the risk of tumor underdosage, and ITV should be considered as a safer option in these specific conditions.

In conclusion, compared to the conventional ITV, the MidP strategy significantly reduced the PTV and the irradiated volumes in all patients, with potential room for dose escalation protocols. Furthermore, MidP proved to be feasible and safe in helical delivery for a representative set of patients commonly treated by radiation therapy and with lung tumors whose stage ranged from early to locally advanced. However, patients having very small tumors with large amplitude motions must be treated cautiously; the conventional ITV remains safer in this particular case.

Conflict of interest

The authors declare they have no conflict of interest.

Acknowledgements

This research program was supported by a grant from the Belgian national fund for scientific research (FRS-FNRS Télévie, grant number, 7.4537.09). E. Sterpin is a Research Fellow with the FRS-FNRS (FC 73512). X. Geets is a Postdoctoral Researcher with the FRS-FNRS, partly funded by the Clinical and Experimental Research Institute (IREC). John A. Lee is a Research Associate with the FRS-FNRS (FC 63880).

Appendix A. Supplementary data

Supplementary data associated with this article can be found, in the online version, at http://dx.doi.org/10.1016/j.radonc.2013.10.025.

References

[1] Guckenberger M, Kavanagh A, Webb S, Brada M. A novel respiratory motion compensation strategy combining gated beam delivery and mean target position concept –a compromise between small safety margins and long duty cycles. Radiother Oncol 2011;98:317–22.
[2] van der Voort van Zyp NC, Prevost JB, Hoogeman MS, et al. Stereotactic radiotherapy with real-time tumor tracking for non-small cell lung cancer: clinical outcome. Radiother Oncol 2009;91:296–300.
[3] Sterpin E, Janssens G, Orban de Xivry J, et al. Helical tomotherapy for SIB and hypo-fractionated treatments in lung carcinomas: a 4D Monte Carlo treatment planning study. Radiother Oncol 2012;104:173–80.
[4] Ekberg L, Holmberg O, Wittgren L, Bjelkengren G, Landberg T. What margins should be added to the clinical target volume in radiotherapy treatment planning for lung cancer? Radiother Oncol 1998;48:71–7.
[5] Keall PJ, Mageras GS, Balter JM, et al. The management of respiratory motion in radiation oncology report of AAPM Task Group 76. Med Phys 2006;33:3874–900.
[6] Liu HH, Balter P, Tutt T, et al. Assessing respiration-induced tumor motion and internal target volume using four-dimensional computed tomography for radiotherapy of lung cancer. Int J Radiat Oncol Biol Phys 2007;68:531–40.
[7] Mutaf YD, Brinkmann DH. Optimization of internal margin to account for dosimetric effects of respiratory motion. Int J Radiat Oncol Biol Phys 2008;70:1561–70.
[8] Wolthaus JW, Sonke JJ, van Herk M, et al. Comparison of different strategies to use four-dimensional computed tomography in treatment planning for lung cancer patients. Int J Radiat Oncol Biol Phys 2008;70:1229–38.
[9] van Herk M, Remeijer P, Rasch C, Lebesque JV. The probability of correct target dosage: dose–population histograms for deriving treatment margins in radiotherapy. Int J Radiat Oncol Biol Phys 2000;47:1121–35.
[10] Kruis MF, van de Kamer JB, Sonke JJ, van Jansen EP, Herk M. Registration accuracy and image quality of time averaged mid-position CT scans for liver SBRT. Radiother Oncol 2013;109:404–8.
[11] Wolthaus JW, Sonke JJ, van Herk M, Damen EM. Reconstruction of a time-averaged midposition CT scan for radiotherapy planning of lung cancer patients using deformable registration. Med Phys 2008;35:3998–4011.
[12] Janssens G, Jacques L, Orban de Xivry J, Geets X, Macq B. Diffeomorphic registration of images with variable contrast enhancement. Int J Biomed Imaging 2011;2011:891585.
[13] Hurkmans CW, Cuijpers JP, Lagerwaard FJ, et al. Recommendations for implementing stereotactic radiotherapy in peripheral stage IA non-small cell lung cancer: report from the Quality Assurance Working Party of the randomised phase III ROSEL study. Radiat Oncol 2009;4:1.
[14] Potters L, Kavanagh B, Galvin JM, et al. American Society for Therapeutic Radiology and Oncology (ASTRO) and American College of Radiology (ACR) practice guideline for the performance of stereotactic body radiation therapy. Int J Radiat Oncol Biol Phys 2010;76:326–32.
[15] Geets X, Lee JA, Bol A, Lonneux M, Gregoire V. A gradient-based method for segmenting FDG-PET images: methodology and validation. Eur J Nucl Med Mol Imaging 2007;34:1427–38.
[16] Wanet M, Lee JA, Weynand B, et al. Gradient-based delineation of the primary GTV on FDG-PET in non-small cell lung cancer: a comparison with threshold-based approaches, CT and surgical specimens. Radiother Oncol 2011;98:117–25.
[17] Bissonnette JP, Franks KN, Purdie TG, et al. Quantifying interfraction and intrafraction tumor motion in lung stereotactic body radiotherapy using respiration-correlated cone beam computed tomography. Int J Radiat Oncol Biol Phys 2009;75:688–95.
[18] Sonke JJ, van Lebesque J, Herk M. Variability of four-dimensional computed tomography patient models. Int J Radiat Oncol Biol Phys 2008;70:590–8.
[19] Wolthaus JW, Schneider C, Sonke JJ, et al. Mid-ventilation CT scan construction from four-dimensional respiration-correlated CT scans for radiotherapy planning of lung cancer patients. Int J Radiat Oncol Biol Phys 2006;65:1560–71.
[20] Witte MG, van der Geer J, Schneider C, van Lebesque JV, Herk M. The effects of target size and tissue density on the minimum margin required for random errors. Med Phys 2004;31:3068–79.
[21] Orban de Xivry J, Janssens G, Bosmans G, et al. Tumour delineation and cumulative dose computation in radiotherapy based on deformable registration of respiratory correlated CT images of lung cancer patients. Radiother Oncol 2007;85:232–8.
[22] van Baardwijk A, Bosmans G, Bentzen SM, et al. Radiation dose prescription for non-small-cell lung cancer according to normal tissue dose constraints: an in silico clinical trial. Int J Radiat Oncol Biol Phys 2008;71:1103–10.
[23] Prescribing, recording, and reporting intensity-modulated photon-beam therapy (IMRT). ICRU report 83, Journal of the ICRU, Vol. 10, No. 1.
[24] Timmerman R, Galvin J, Michalski J, et al. Accreditation and quality assurance for Radiation Therapy Oncology Group: Multicenter clinical trials using Stereotactic Body Radiation Therapy in lung cancer. Acta Oncol 2006;45:779–86.
[25] Xiao Y, Papiez L, Paulus R, et al. Dosimetric evaluation of heterogeneity corrections for RTOG 0236: stereotactic body radiotherapy of inoperable stage I-II non-small-cell lung cancer. Int J Radiat Oncol Biol Phys 2009;73:1235–42.
[26] Ardu V, Broggi S, Cattaneo GM, Mangili P, Calandrino R. Dosimetric accuracy of tomotherapy dose calculation in thorax lesions. Radiat Oncol 2011;6:14.
[27] Chen Q, Lu W, Chen Y, Chen M, Henderson D, Sterpin E. Validation of GPU based TomoTherapy dose calculation engine. Med Phys 2012;39:1877–86.
[28] Admiraal MA, Schuring D, Hurkmans CW. Dose calculations accounting for breathing motion in stereotactic lung radiotherapy based on 4D-CT and the internal target volume. Radiother Oncol 2008;86:55–60.
[29] Guckenberger M, Wilbert J, Krieger T, et al. Four-dimensional treatment planning for stereotactic body radiotherapy. Int J Radiat Oncol Biol Phys 2007;69:276–85.

[30] Han K, Basran PS, Cheung P. Comparison of helical and average computed tomography for stereotactic body radiation treatment planning and normal tissue contouring in lung cancer. Clin Oncol (R Coll Radiol) 2010;22:862–7.
[31] Bradley J, Graham MV, Winter K, et al. Toxicity and outcome results of RTOG 9311: a phase I–II dose–escalation study using three-dimensional conformal radiotherapy in patients with inoperable non-small-cell lung carcinoma. Int J Radiat Oncol Biol Phys 2005;61:318–28.
[32] Bradley JD, Moughan J, Graham MV, et al. A phase I/II radiation dose escalation study with concurrent chemotherapy for patients with inoperable stages I to III non-small-cell lung cancer: phase I results of RTOG 0117. Int J Radiat Oncol Biol Phys 2010;77:367–72.
[33] Gagliardi G, Constine LS, Moiseenko V, et al. Radiation dose–volume effects in the heart. Int J Radiat Oncol Biol Phys 2010;76:S77–85.
[34] Kong FM, Ten Haken RK, Schipper MJ, et al. High-dose radiation improved local tumor control and overall survival in patients with inoperable/unresectable non-small-cell lung cancer: long-term results of a radiation dose escalation study. Int J Radiat Oncol Biol Phys 2005;63:324–33.
[35] Marks LB, Bentzen SM, Deasy JO, et al. Radiation dose–volume effects in the lung. Int J Radiat Oncol Biol Phys 2010;76:S70–6.
[36] Shi A, Zhu G, Wu H, Yu R, Li FXuB. Analysis of clinical and dosimetric factors associated with severe acute radiation pneumonitis in patients with locally advanced non-small cell lung cancer treated with concurrent chemotherapy and intensity-modulated radiotherapy. Radiat Oncol 2010;5:35.
[37] Socinski MA, Morris DE, Halle JS, et al. Induction and concurrent chemotherapy with high-dose thoracic conformal radiation therapy in unresectable stage IIIA and IIIB non-small-cell lung cancer: a dose–escalation phase I trial. J Clin Oncol 2004;22:4341–50.
[38] Song CH, Pyo H, Moon SH, Kim TH, Kim DW, Cho KH. Treatment-related pneumonitis and acute esophagitis in non-small-cell lung cancer patients treated with chemotherapy and helical tomotherapy. Int J Radiat Oncol Biol Phys 2010;78:651–8.
[39] van Baardwijk A, Wanders S, Boersma L, et al. Mature results of an individualized radiation dose prescription study based on normal tissue constraints in stages I to III non-small-cell lung cancer. J Clin Oncol 2010;28:1380–6.
[40] Werner-Wasik M, Yorke E, Deasy J, Nam J, Marks LB. Radiation dose–volume effects in the esophagus. Int J Radiat Oncol Biol Phys 2010;76:S86–93.
[41] van Elmpt W, De Ruysscher D, van der Salm A, et al. The PET-boost randomised phase II dose–escalation trial in non-small cell lung cancer. Radiother Oncol 2012;104:67–71.
[42] Bortfeld T, Jokivarsi K, Goitein M, Kung J, Jiang SB. Effects of intra-fraction motion on IMRT dose delivery: statistical analysis and simulation. Phys Med Biol 2002;47:2203–20.
[43] Sterpin E, Hundertmark BT, Mackie TR, Lu W, Olivera GH, Vynckier S. Monte Carlo-based analytical model for small and variable fields delivered by TomoTherapy. Radiother Oncol 2010;94:229–34.
[44] Sterpin E, Salvat F, Olivera G, Vynckier S. Monte Carlo evaluation of the convolution/superposition algorithm of Hi-Art tomotherapy in heterogeneous phantoms and clinical cases. Med Phys 2009;36:1566–75.
[45] Sterpin E, Salvat F, Cravens R, Ruchala K, Olivera GH, Vynckier S. Monte Carlo simulation of helical tomotherapy with PENELOPE. Phys Med Biol 2008;53:2161–80.
[46] Sterpin ETM, Cravens R, et al. Monte Carlo simulation of the Tomotherapy treatment unit in the static mode using MC HAMMER a Monte Carlo tool dedicated to Tomotherapy. J Phys: Confer Ser 2007;74:021019.
[47] Zhao YL, Mackenzie M, Kirkby C, Fallone BG. Monte Carlo evaluation of a treatment planning system for helical tomotherapy in an anthropomorphic heterogeneous phantom and for clinical treatment plans. Med Phys 2008;35:5366–74.
[48] Paddick I. A simple scoring ratio to index the conformity of radiosurgical treatment plans. Technical note. J Neurosurg 2000;93:219–22.
[49] Wu QR, Wessels BW, Einstein DB, Maciunas RJ, Kim EY, Kinsella TJ. Quality of coverage: conformity measures for stereotactic radiosurgery. J Appl Clin Med Phys 2003;4:374–81.
[50] Dice LR. Measures of the amount of ecologic association between species. Ecology 1945;26:297–302.
[51] Kissick MW, Flynn RT, Westerly DC, et al. On the impact of longitudinal breathing motion randomness for tomotherapy delivery. Phys Med Biol 2008;53:4855–73.
[52] Yang JN, Mackie TR, Reckwerdt P, Deasy JO, Thomadsen BR. An investigation of tomotherapy beam delivery. Med Phys 1997;24:425–36.
[53] Kissick MW, Boswell SA, Jeraj R, Mackie TR. Confirmation, refinement, and extension of a study in intrafraction motion interplay with sliding jaw motion. Med Phys 2005;32:2346–50.
[54] Cao M, Lasley FD, Das IJ, Desrosiers CM, Slessinger ED, Cardenes HR. Evaluation of rotational errors in treatment setup of stereotactic body radiation therapy of liver cancer. Int J Radiat Oncol Biol Phys 2012;84:e435–40.
[55] Guckenberger M, Meyer J, Vordermark D, Baier K, Wilbert J, Flentje M. Magnitude and clinical relevance of translational and rotational patient setup errors: a cone-beam CT study. Int J Radiat Oncol Biol Phys 2006;65:934–42.
[56] Schubert LK, Westerly DC, Tome WA, et al. A comprehensive assessment by tumor site of patient setup using daily MVCT imaging from more than 3,800 helical tomotherapy treatments. Int J Radiat Oncol Biol Phys 2009;73:1260–9.

Please cite this article in press as: Wanet M et al. Validation of the mid-position strategy for lung tumors in helical TomoTherapy. Radiother Oncol (2014), http://dx.doi.org/10.1016/j.radonc.2013.10.025